Synergistic effects of Akebia saponin D and Semaglutide on diabetic nephropathy and osteoporosis via the Klotho-p53 signaling axis

QIAN ZHANG, DAN WANG, HONGXIA JIA, ZONGJI ZHENG, LIYAN LIN, LINNA LI, LING WANG and YAOMING XUE

Department of Endocrinology and Metabolism, Nanfang Hospital, Southern Medical University, Guangzhou, Guangdong 510515, P.R. China

Received July 3, 2025; Accepted October 14, 2025

DOI: 10.3892/ijmm.2025.5696

Abstract. Diabetic nephropathy (DN) and diabetic osteoporosis (DOP) are frequent and debilitating complications of diabetes mellitus (DM), sharing pathological features such as oxidative stress, inflammation and metabolic dysregulation. However, current therapies rarely address these comorbidities simultaneously. In the present study, a type 2 DM rat model presenting both DN and DOP characteristics was established. Rats were treated with Akebia saponin D (ASD), Semaglutide, or their combination. Renal function, calcium-phosphate metabolism, bone microarchitecture and mechanical properties were evaluated. Network pharmacology, molecular docking and knockdown validation were employed to elucidate underlying mechanisms. Combination therapy markedly improved glomerular structure, decreased fibrosis, restored trabecular bone volume and strength and corrected metabolic imbalance more effectively than monotherapy. Bioinformatic analysis identified the Klotho-p53 signaling axis as a potential target. ASD exhibited high binding affinity to Klotho in silico and adeno-associated virus-mediated Klotho knockdown reversed therapeutic benefits, confirming its pivotal role. ASD and Semaglutide synergistically alleviated both DN and DOP by modulating the Klotho-p53 axis, offering a promising strategy for comprehensive DM complication management.

Introduction

Diabetes mellitus (DM) is a common chronic metabolic disorder with multifactorial etiology (1). It is characterized by elevated blood glucose levels or hyperglycemia, which results from either insufficient insulin production due to β-cell dysfunction or impaired insulin action secondary to insulin resistance (2). In recent years, the incidence and prevalence of DM have risen sharply due to changes in lifestyle, including prolonged physical inactivity, sedentary behavior and excessive intake of high-fat and high-sugar (HFHS) diets. According to the latest epidemiological data from the International Diabetes Federation, >425 million people worldwide are currently affected by DM, a figure expected to rise to 629 million by 2045 (3), underscoring the growing threat of DM to global health.

Diabetic nephropathy (DN) is one of the most common complications of DM, affecting ~40% of patients with DM throughout disease progression (4). DN is primarily attributed to chronic hyperglycemia-induced microvascular damage in the kidneys, which leads to impaired renal perfusion and subsequently triggers inflammation, oxidative stress, glomerulosclerosis and tubulointerstitial fibrosis, ultimately resulting in progressive and irreversible renal dysfunction. As DN progresses, patients may develop symptoms such as edema, hypertension and proteinuria; in advanced stages, some individuals require dialysis to maintain internal homeostasis, which severely compromises both life expectancy and quality of life (5). Diabetic osteoporosis (DOP) is another common complication of DM, with a complex pathogenesis involving multiple pathophysiological mechanisms, including diminished insulin-mediated inhibition of bone resorption, enhanced bone destruction due to chronic inflammation and local accumulation of advanced glycation end-products in bone tissue (6). The principal complication associated with DOP is fragility fractures. Clinical investigations have shown that individuals with DM are 1.38-1.7 times more likely to sustain proximal femoral fractures and 2.03 times more likely to experience vertebral fractures than healthy individuals (7-9). Although fractures associated with DOP are not directly fatal, they markedly impair the self-care ability of patients with DM, imposing a substantial burden on both patients and their families. More importantly, there appears to be a potential link between DN and DOP, two major complications of DM. A study by Xia *et al* (10) demonstrated that patients with DN are at markedly higher risk of developing DOP compared with those with DM without DN. Conversely, a case-control study

Correspondence to: Dr Yaoming Xue, Department of Endocrinology and Metabolism, Nanfang Hospital, Southern Medical University, 1838 Guangzhou Avenue North, Guangzhou, Guangdong 510515, P.R. China
E-mail: xueyaoming999@126.com

Key words: Akebia saponin D, Semaglutide, diabetic nephropathy, diabetic osteoporosis, Klotho-p53 signaling axis

by Yan *et al* (11) identified osteoporosis (OS) as an independent risk factor for DN among patients with DM. These findings indicate that treatment strategies for DM must consider both kidney and bone status to prevent the reciprocal exacerbation between DN and DOP, a key step toward improving clinical outcomes and extending patient lifespan.

Akebia saponin D (ASD), a natural small-molecule bioactive compound isolated from *Dipsacus asper*, exhibits multiple pharmacological properties, including anti-inflammatory, antioxidant and anti-apoptotic effects (12). Previous cellular and animal studies have demonstrated the therapeutic potential of ASD in diseases such as bronchial asthma, cerebral hemorrhage and hepatic steatosis (13-15). However, the efficacy of ASD in treating DM complications remains largely unexplored.

Semaglutide, a long-acting glucagon-like peptide-1 (GLP-1) receptor agonist, has been widely used in clinical practice for the management of type 2 DM (T2DM) (16). Specifically, Semaglutide facilitates glycemic control and weight reduction in patients with T2DM by enhancing insulin secretion, suppressing glucagon release, delaying gastric emptying and improving insulin sensitivity (17). However, the therapeutic potential and underlying mechanisms of Semaglutide in DN and DOP remain inadequately elucidated.

Accordingly, the present study intended to construct a dual-complication DM rat model characterized by both DN and DOP using high-fat feeding and repeated low-dose streptozotocin (STZ) injections. ASD, selected for its documented anti-inflammatory, antioxidant and anti-apoptotic properties and its potential benefits in metabolic disorders and Semaglutide were then administered to the animals to comprehensively assess their combined efficacy in improving DN and DOP, as well as to explore the potential mechanisms involved. It was hypothesized that ASD and Semaglutide may exert synergistic protective effects against DN and DOP by modulating the Klotho-p53 signaling axis. The outcomes of this research may provide a theoretical basis for the combined use of ASD and Semaglutide and contribute novel perspectives on the management of DM complications.

Materials and methods

Experimental animals. A total of 42 male Sprague-Dawley rats (SPF grade; 180-220 g; 8 weeks old) were provided by Guangdong Medical Laboratory Animal Center [Production License No. SCXK (Yue) 2022-0002]. Only male rats were used in order to avoid the potential variability associated with the estrous cycle in females, which could influence glucose metabolism, bone turnover and renal function (18,19). This approach was chosen to minimize hormonal fluctuations and ensure experimental consistency. Rats were housed under controlled conditions (20-26˚C; 30-70% humidity; 12 h light/dark cycle) with free access to food and water. Ethical approval for the present study was obtained from the Animal Welfare and Ethics Committee of Guangdong Medical Laboratory Animal Center (approval no. D202505-13).

Reagents, virus construction and animal grouping. STZ, ASD and Semaglutide were obtained from MedChemExpress and the chemical structures of ASD and Semaglutide are shown in Fig. 1A and B. STZ (30 mg/kg) was freshly prepared in 0.1 M sodium citrate buffer (pH 4.5) and administered intraperitoneally once daily for two consecutive days. ASD (90 mg/kg/day) was dissolved in DMSO (Beijing Solarbio Science & Technology Co., Ltd.) and diluted with PBS (Beijing Solarbio Science & Technology Co., Ltd.; pH 7.4) for oral gavage, with a final volume of 10 ml/kg. Semaglutide (120 μg/kg/day, subcutaneous injection, 12 weeks) was dissolved in PBS(pH 7.4) and administered subcutaneously at a dose volume of 1 ml/kg (20). The dosage was selected based on previous clinical and preclinical studies demonstrating safe and effective exposure (21,22). A formal dose-response trial was not conducted in the present study. All doses were adjusted according to body surface area to ensure pharmacological equivalence (23). To silence Klotho expression, a recombinant adeno-associated virus (AAV) encoding either Klotho-specific short hairpin (sh)RNA (sh-Klotho) or non-targeting control shRNA (shNC) was synthesized by Shanghai GenePharma Co., Ltd. Viral particles were prepared using standard protocols and purified by polyethylene glycol precipitation and ultracentrifugation and administered via tail vein injection (200 μl/injection) every three days.

Following one week of acclimatization, the rats were randomly assigned into seven groups (n=6 per group). During the modeling process, two rats in the MOD group and one rat in the M + S group died and one rat in the MOD group did not meet the diabetic criteria (fasting blood glucose <7.8 mmol/l). Thus, the final numbers of rats analyzed were: Control (n=6), MOD (n=3), M + A (n=6), M + S (n=5), M + A + S (n=6), M + A + S + shNC (n=6) and M + A + S + sh-Klotho (n=6). A T2DM model was established based on previously validated methods (24-26), involving high-fat high-sucrose (HFHS) feeding for 8 weeks followed by two consecutive low-dose intraperitoneal injections of streptozotocin (STZ; 30 mg/kg). This combination is widely recognized as a reliable method to induce T2DM-like phenotypes, as it produces insulin resistance with partial β-cell dysfunction rather than complete β-cell destruction typical of type 1 diabetes (T1DM). Rats with fasting blood glucose (FBG) >7.8 mmol/l and reduced insulin sensitivity were considered successfully modeled. The experimental groups were as follows: i) Control: Standard diet + vehicle (sodium citrate buffer, i.p.) + saline via oral gavage for 12 weeks. ii) Model (MOD): HFHS diet + STZ + saline via oral gavage for 12 weeks. iii) MOD + ASD (M + A): MOD model + ASD via oral gavage for 12 weeks. iv) MOD + Semaglutide (M + S): MOD model + Semaglutide via subcutaneous injection for 12 weeks. v) MOD + ASD + Semaglutide (M + A + S): Combined ASD (oral gavage) and Semaglutide (subcutaneous) for 12 weeks. vi) M + A + S + shNC: Same as group 5, plus tail vein injection of AAV-shNC every three days. vii) M + A + S + sh-Klotho: Same as group 5, plus tail vein injection of AAV-shKlotho every three days. The ASD dose used in the present study was referenced from the research by Yu *et al* (27), while the Semaglutide dose was based on the clinically recommended safe and effective dosage (21,22).

Sample collection and processing. After the final treatment, rats were placed in PhenoMaster metabolic cages (TSE Systeme GmbH) for 24 h, with free access to water but no food. Urine was collected, centrifuged (1,000 x g; 5 min;

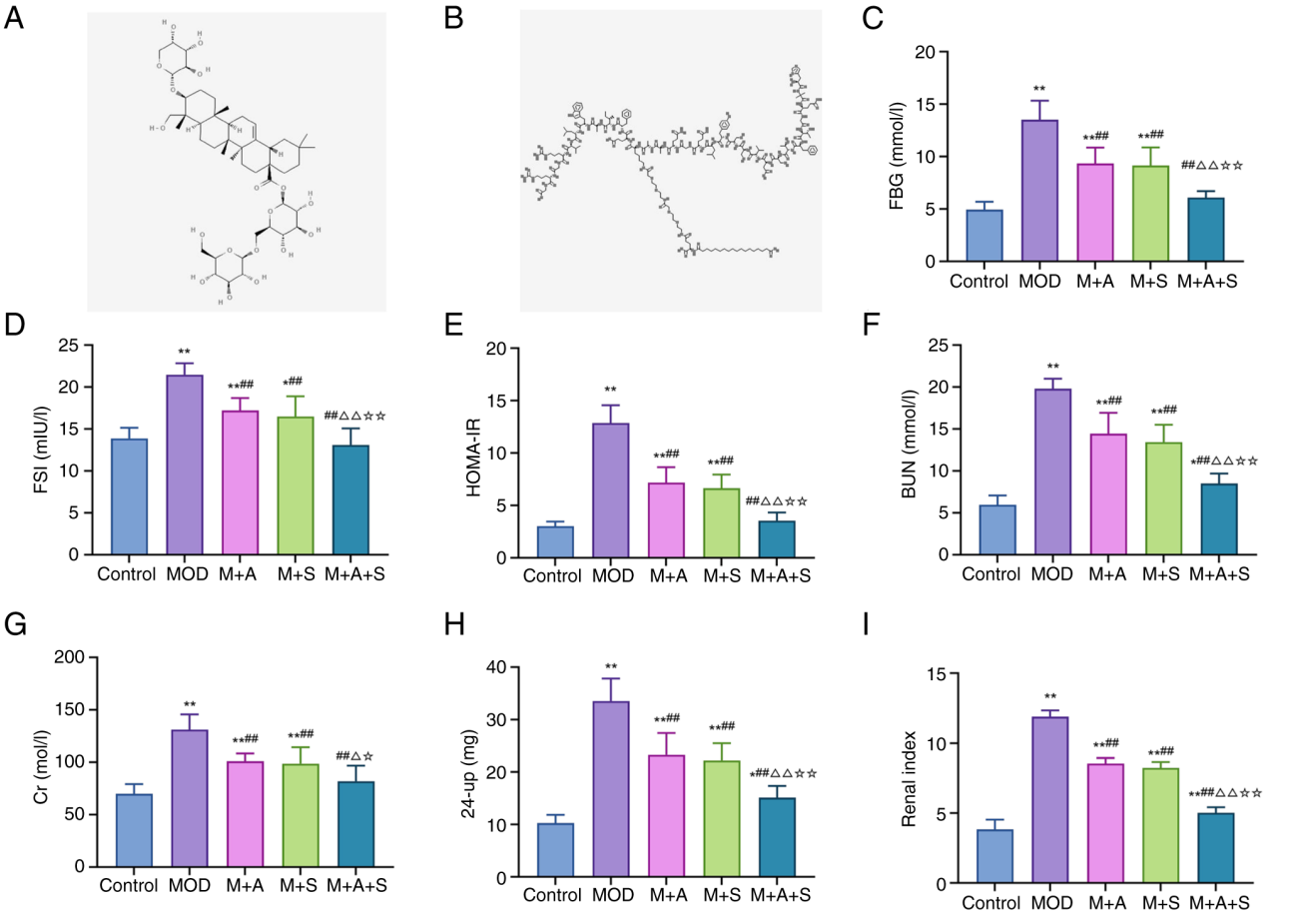

Figure 1. Chemical structures of ASD and Semaglutide and their effects on glucose metabolism and renal function in diabetic rats. Two-dimensional structures of (A) ASD and (B) Semaglutide were retrieved from PubChem. Enzyme-linked immunosorbent assay analysis of (C) FBG, (D) FSI and (E) HOMA-IR. (F-I) Biochemical analysis of BUN, Cr, 24-up and renal index. *P<0.05, **P<0.01 vs. Control; $^{\#\#}$P<0.01 vs. MOD; $^{\triangle}$P<0.05, $^{\triangle\triangle}$P<0.01 vs. M + A; *P<0.05, **P<0.01 vs. M + S. ASD, akebia saponin D; FBG, fasting blood glucose; FSI, fasting serum insulin; HOMA-IR, homeostatic model assessment of insulin resistance; BUN, blood urea nitrogen; Cr, creatinine; 24-up, 24-h urinary protein.

4˚C) and supernatant was analyzed for protein concentration using a BCA kit (Shanghai Lianshui Biotechnology Co., Ltd.). Results were recorded as 24-h urinary protein (24 up) levels. The following morning, rats were anesthetized and sacrificed by intraperitoneal injection of sodium pentobarbital at a dose of 150 mg/kg. Body and kidney weights were measured to calculate the renal index (kidney weight/body weight). Blood samples were collected via abdominal aorta, centrifuged (1,500 x g; 5 min; 4˚C) and serum stored at -80˚C. Both kidneys and femurs were harvested under sterile conditions, cleared of soft tissues and stored at -80˚C for further analysis.

Biochemical analysis. The femoral tissues were defatted, crushed and acid-digested. Serum, urine and femur extracts were analyzed for blood urea nitrogen (BUN), creatinine (Cr), calcium (Ca^{2+}) and phosphate (PO_4^{3-}) levels using a HITACHI-7170S automatic biochemical analyzer (Hitachi High-Technologies Corporation). Serum levels of glycometabolic and bone turnover markers were measured using commercial enzyme-linked immunosorbent assay (ELISA) kits. Glycometabolic indicators included fasting blood glucose (FBG; cat. no. E02G0462; Shanghai BlueGene Biotech), fasting serum insulin (FSI; cat. no. mlE2721; Shanghai Enzyme-linked Biotechnology Co., Ltd.). The homeostatic model assessment of insulin resistance (HOMA-IR), which was calculated using the formula: HOMA-IR=(FBG x FSI)/22.5. This calculation was used to indirectly evaluate insulin sensitivity in the diabetic rat model. Bone turnover markers were quantified using rat ELISA kits from Shanghai Enzyme-linked Biotechnology Co., Ltd: alkaline phosphatase (ALP; cat. no. ml107021), procollagen type I N-terminal propeptide (PINP; cat. no. ml038224-1), C-terminal telopeptide of type I collagen (CTX-I; cat. no. ml003410) and tartrate-resistant acid phosphatase (TRAP; cat. no. ml059485). Each assay was performed in triplicate.

Histological analysis of kidney and femur tissues. After fixation in 4% paraformaldehyde solution for 24 h at 4˚C, kidney and femur tissues were embedded in paraffin and sectioned into 4-μm slices using a microtome (Leica Biosystems). Kidney sections were made in the coronal plane and femur sections along the longitudinal axis. Sections were deparaffinized in xylene and rehydrated through graded ethanol solutions (28). Hematoxylin and eosin (H&E) staining was performed to assess renal and femoral structural integrity. The glomerulosclerosis index (GSI) and renal tubular interstitial injury index (RTI) were calculated according to previous studies (29). In femoral sections, osteoblasts and osteocytes were quantified.

Additional staining included periodic acid-Schiff (PAS) for glomerular basement membrane injury: 0.5% periodic acid for 10 min at room temperature (RT), Schiff reagent 15 min, two sulfite washes (5 min each), and hematoxylin counterstain 2 min, followed by dehydration, clearing, and mounting. Masson's trichrome was performed for renal fibrosis evaluation: Bouin's solution 56˚C, 30 min, Weigert's iron hematoxylin 10 min, Biebrich scarlet-acid fuchsin 10 min, phosphomolybdic/phosphotungstic acid 10 min, aniline blue 10 min, and 1% acetic acid 2 min, followed by dehydration, clearing and mounting. Images were acquired an Olympus BX53 microscope (Olympus Corporation) and quantified using ImageJ v1.53 (NIH) based on three randomly selected fields per section.

Micro-computed tomography (micro-CT) analysis. Femoral microarchitecture was assessed by SkyScan 1276 micro-CT (Bruker Corporation). Scanning parameters included 300 μA tube current, 75 kV tube voltage, 75 msec exposure time, 0.7˚ rotation step and 12 μm voxel resolution, averaging 2 frames per step. Images were reconstructed with NRecon (version 1.7.4.6; Bruker Corporation) software and the region of interest was defined as a 2.4 mm volume of trabecular bone starting 1 mm proximal to the distal growth plate. Quantitative analysis using CTAn (version 1.20.3.0; ROI) software included measurements of bone mineral density (BMD), bone mineral content (BMC), bone volume/tissue volume (BV/TV), bone surface/bone volume (BS/BV), trabecular separation (Tb.Sp), trabecular thickness (Tb.Th), trabecular number (Tb.N) and structure model index (SMI).

Three-point bending test. Femoral biomechanical properties were evaluated using an RGWF4005 electronic universal testing machine (Shenzhen Reger Instrument Co. Ltd.) after micro-CT scanning. During testing, the distal and proximal ends of the femur were fixed on two support points spaced 10 mm apart and a vertical downward force was applied to the midshaft of the femur until fracture occurred. The ultimate load, bending strength and Young's modulus were recorded to evaluate mechanical integrity.

Immunofluorescence staining. Paraffin-embedded kidney and femur sections (4 μm; prepared as aforementioned) were baked at 60˚C for 30-60 min before staining. Paraffin sections were subjected to heat-induced antigen retrieval in 0.01 M sodium citrate buffer (pH 6.0) at 95˚C, followed by blocking with 3% BSA (MilliporeSigma) for 1 h. Sections were incubated overnight at 4˚C with primary antibodies anti-Klotho (1:200; cat. no. PA5-21078), anti-p53 (1:200; cat. no. MA5-12453) and anti-γ-H2AX (1:200; cat. no. MA5-33062), all from Invitrogen (Thermo Fisher Scientific, Inc.). After primary incubation, slides were washed in PBST (3x5 min), incubated with fluorophore-conjugated secondary antibodies for 1 h at RT, and washed again in PBST (3x5 min). Nuclei were counterstained with DAPI (1 μg/ml, 5 min, RT; protected from light), rinsed in PBS, and mounted with anti-fade medium. Images were captured from three random fields on an Olympus fluorescence microscope (Olympus Corporation) using 10x, 20x, and 40x objectives (identical acquisition settings across groups), and fluorescence intensities were quantified using ImageJ v1.53 (NIH).

Western blot analysis. Total protein was extracted from bilateral residual kidney and femur tissues using RIPA lysis buffer (Cell Signaling Technology, Inc.) supplemented with protease and phosphatase inhibitors. Protein concentrations were determined using a BCA protein assay kit (Beyotime Biotechnology) and 30 μg protein per lane was loaded. Equal amounts of protein were separated by 10% SDS-PAGE (Bio-Rad Laboratories, Inc.), transferred to polyvinylidene fluoride (PVDF) membranes (Wuhan Servicebio Technology Co., Ltd.) and blocked in 5% non-fat milk for 1 h at room temperature. Membranes were then incubated overnight at 4˚C with the following primary antibodies (all from Invitrogen; Thermo Fisher Scientific, Inc.): TGF-β1 (cat. no. MA5-16949; 1:1,000), α-smooth muscle actin (α-SMA; cat. no. 14-9760-82; 1:1,000), Collagen I (cat. no. PA1-26204; 1:1,000), Collagen IV (cat. no. PA5-104508; 1:1,000), osteoprotegerin (OPG; cat. no. MA5-15715; 1:1,000), osteocalcin (OCN; cat. no. MA1-20786; 1:1,000), receptor activator of nuclear factor κ-b ligand (RANKL; cat. no. MA1-41161; 1:1,000), Runt-related transcription factor 2 (RUNX2; cat. no. PA5-82787; 1:1,000), Klotho (cat. no. MA5-32784, 1:1,000), γ-Histone H2AX (γ-H2AX; cat. no. MA5-33062, 1:1,000), ataxia-telangiectasia mutated protein (ATM; cat. no. MA1-23152; 1:1,000), phosphorylated (p-)ATM (cat. no. MA1-2020; 1:1,000), p53 (vMA5-12557; 1:1,000), p21 (cat. no. MA5-14949, 1:1,000) and GAPDH (vMA5-15738; 1:5,000). After TBST washes, HRP-conjugated secondary antibodies (cat. nos. 32460 and 62-6520; 1:10,000; Thermo Fisher Scientific, Inc.) were applied for 1 h at room temperature. Bands were visualized using an ECL chemiluminescent substrate (SuperSignal West Pico PLUS, Thermo Fisher Scientific, Inc.) and imaged on a Tanon 5200 system (Tanon Science and Technology Co., Ltd.). Densitometry was performed using ImageJ v1.53 (NIH), and target signals were normalized to GAPDH. Each sample was analyzed in triplicate.

Bioinformatics analysis. Transcriptomic datasets related to DN and OS were obtained from the Gene Expression Omnibus (GEO) (https://www.ncbi.nlm.nih.gov/geo/) (GSE30528 and GSE35958). Data were downloaded using GEOquery (v2.70.0; Bioconductor; https://bioconductor.org/packages/GEOquery) in R (v4.3.2; The R Foundation; https://www.r-project.org/), normalized and batch-corrected with limma (v3.58.1; Bioconductor; https://bioconductor.org/packages/limma) and differentially expressed genes (DEGs) were identified using DESeq2. Targets of ASD and Semaglutide were retrieved from ChEMBL (https://www.ebi.ac.uk/chembl), intersected with DEGs related to DN and OS. Gene Ontology (GO) and Kyoto Encyclopedia of Genes and Genomes (KEGG) enrichment analyses were conducted via ClusterProfiler to explore biological functions and pathways. Protein structures were downloaded from the Protein Data Bank (https://www.rcsb.org/) and compound structures from PubChem (https://pubchem.ncbi.nlm.nih.gov/). Docking was performed in AutoDock Vina (The Scripps Research Institute) and visualized using PyMOL v2.5.4 (https://www.pymol.org/).

Statistical analysis. Statistical analyses were performed using SPSS 24.0 (IBM Corp.). The Shapiro-Wilk test and Levene's test were applied to assess normality and homogeneity of

variances. If the data met these assumptions, one-way ANOVA followed by Tukey's post hoc test was conducted. Data were presented as mean ± standard deviation (SD). $P<0.05$ was considered to indicate a statistically significant difference.

Results

ASD and Semaglutide improve glucose metabolism and renal function in diabetic rats. Abnormal glucose metabolism and impaired renal filtration and barrier functions are key features of DM and DN. To evaluate the pharmacological effects of ASD and Semaglutide, the present study first assessed metabolic and renal indicators.

ELISA results showed that the levels of FBG, FSI and HOMA-IR in the MOD group were markedly higher than those in the Control group. However, treatment with ASD or Semaglutide alone (M + A/M + S group) reduced these markers and the combined therapy (M + A + S group) led to the most significant improvement (Fig. 1C-E). Similarly, biochemical analysis revealed that the levels of BUN, Cr, 24-up and renal index were markedly increased in the MOD group. All parameters were markedly decreased following treatment, with the M + A + S group showing superior renoprotection (Fig. 1F-I). These findings suggested that ASD and Semaglutide together improve glucose homeostasis and attenuate renal dysfunction in diabetic rats, with combination therapy outperforming monotherapy. Although body weight after 6 weeks of HFHS feeding was not recorded in the present study, previous reports using the same modeling protocol have consistently shown an initial increase in body weight during HFHS feeding followed by a moderate decline after STZ injection, reflecting typical T2DM progression rather than T1DM (25).

ASD and Semaglutide alleviate renal pathological damage in diabetic rats. Kidney injury in DN involves both functional impairment and structural abnormalities. To assess the histopathological improvements following treatment, H&E, PAS and Masson staining were performed.

H&E staining (Fig. 2A) revealed pronounced glomerular hypertrophy, basement membrane thickening, mesangial expansion and inflammatory infiltration in the MOD group. The two monotherapies partly alleviated these lesions, while the M + A + S group demonstrated the most comprehensive improvement, as reflected by markedly reduced GSI and RTI scores (Fig. 2B and C). PAS staining (Fig. 2D and E) showed marked glomerular and tubular basement membrane thickening in the MOD group, along with prominent PAS-positive deposits. Treatment reversed these changes, with the M + A + S group achieving the greatest reduction in PAS-positive area. Masson staining (Fig. 2F and G) showed extensive collagen deposition in MOD rats, which was markedly reduced after treatment. The collagen area percentage was lowest in the M + A + S group, indicating superior antifibrotic efficacy. At the molecular level, western blot analysis (Fig. 2H and I) confirmed significant upregulation of TGF-β1, α-SMA, Collagen I and Collagen IV in the MOD group. These profibrotic markers were markedly downregulated by combination therapy, with levels approaching those of the Control group.

Collectively, these findings demonstrated that ASD and Semaglutide synergistically attenuate renal injury, reduce basement membrane thickening and suppress renal fibrosis, with the combination therapy yielding superior outcomes compared with monotherapy.

ASD and Semaglutide improve calcium and phosphate metabolism in diabetic rats. Disrupted calcium and phosphate metabolism is a common feature of internal environment disturbance in patients with DM and may play an important role in DM-related renal injury and OS (30). Therefore, the levels of Ca^{2+} and PO_4^{3-} in serum, urine and femur were measured in the present study to evaluate the therapeutic effects of ASD and Semaglutide. As shown in Fig. 3A-F, the MOD group exhibited markedly elevated serum PO_4^{3-} (Fig. 3B), increased urinary excretion of Ca^{2+} and PO_4^{3-} (Fig. 3C and D) and reduced femoral Ca^{2+} and PO_4^{3-} content (Fig. 3E and F), indicating systemic calcium-phosphate imbalance. Treatment with either ASD or Semaglutide partly restored these parameters, while the combined treatment (M + A + S) achieved the most substantial correction, including normalization of serum phosphate, reduction in renal loss and restoration of bone mineral content. In summary, these findings suggested that ASD and Semaglutide synergistically restore mineral homeostasis in diabetic rats, with combination therapy demonstrating superior efficacy.

ASD and Semaglutide alleviate diabetic osteoporosis-related femoral damage. DOP is characterized by reduced trabecular bone, decreased bone density and disrupted bone structure (31). To evaluate structural changes, H&E staining and micro-CT were performed.

H&E staining (Fig. 4A) revealed sparse, thinned and disorganized trabeculae in MOD rats. Treatment with ASD or Semaglutide partially improved trabecular integrity, while the combined group (M + A + S) showed the most substantial recovery, as confirmed by markedly higher osteocyte counts (Fig. 4B). Micro-CT analysis (Fig. 4C and D) demonstrated that MOD rats had markedly lower BMD, BMC, BV/TV, Tb.Th and Tb.N, accompanied by elevated BS/BV, Tb.Sp and SMI. These changes reflect weakened and porous bone architecture. All parameters improved following treatment and the M + A + S group exhibited the most pronounced normalization, indicating a synergistic effect of ASD and Semaglutide in preventing DOP-related skeletal deterioration.

ASD and Semaglutide improve bone strength and restore osteogenic-resorptive balance in diabetic rats. DOP is associated with both reduced bone mechanical strength and dysregulated bone metabolism, increasing fracture risk in patients with DM (32,33). In the present study, the effects of ASD and Semaglutide on femoral bone strength, metabolism and remodeling were comprehensively evaluated.

Three-point bending tests revealed that MOD rats exhibited markedly reduced ultimate load, bending strength and elastic modulus, indicating biomechanical fragility. ASD and Semaglutide both improved these parameters, while the combination therapy (M + A + S) led to the most substantial enhancements, suggesting superior restorative effects (Fig. 5A-C).

To further explore underlying mechanisms, serum and tissue markers related to bone formation and resorption

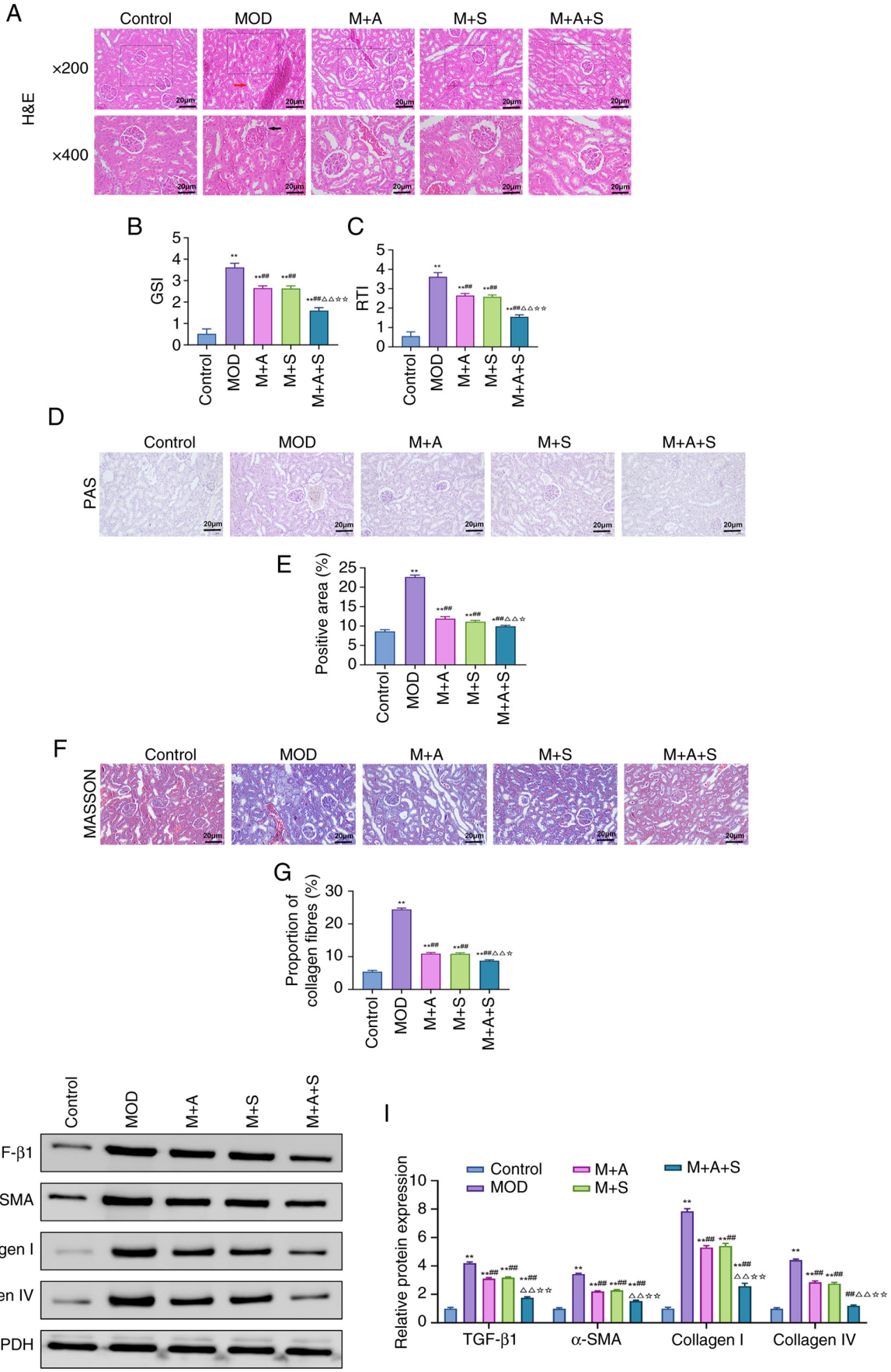

Figure 2. ASD and Semaglutide alleviate renal pathological damage in diabetic rats. (A-C) H&E staining was used to observe kidney structure (magnification, x200 and x400) and perform GSI and RTI scoring. (D) PAS staining and (E) quantification of PAS-positive area. (F) Masson staining and (G) quantification of collagen deposition. (H) Western blot analysis of TGF-β1, α-SMA, Collagen I and Collagen IV. (I) Quantification of protein expression normalized to GAPDH. *P<0.05, **P<0.01 vs. Control; $^{\#\#}$P<0.01 vs. MOD; $^{\triangle}$P<0.05, $^{\triangle\triangle}$P<0.01 vs. M + A; *P<0.05, **P<0.01 vs. M + S. ASD, akebia saponin D; H&E, hematoxylin and eosin; GSI, glomerulosclerosis index; RTI, renal tubular interstitial injury index; PAS, periodic acid-Schiff; α-SMA, α-smooth muscle actin.

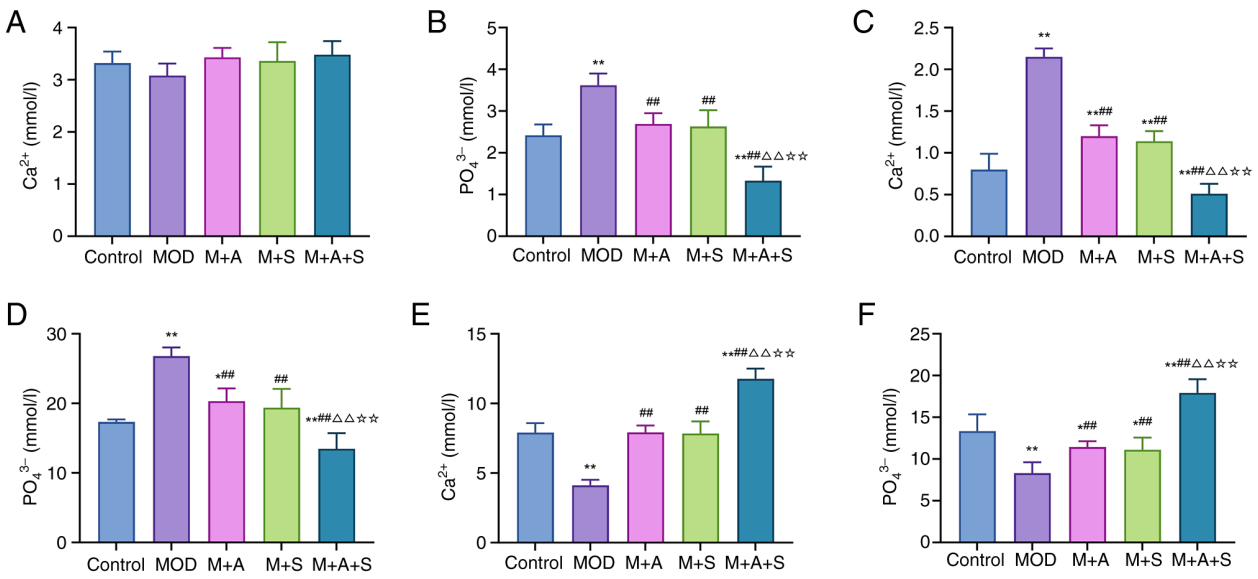

Figure 3. Effects of ASD and Semaglutide on calcium and phosphate metabolism in diabetic rats. (A-F) Biochemical analyzer was used to measure the levels of Ca^{2+} and PO_4^{3-} in (A and B) serum, (C and D) urine and (E and F) femur. *P<0.05, **P<0.01 vs. Control; $^{\#\#}$P<0.01 vs. MOD; $^{\Delta\Delta}$P<0.01 vs. M + A; **P<0.01 vs. M + S. ASD, akebia saponin D.

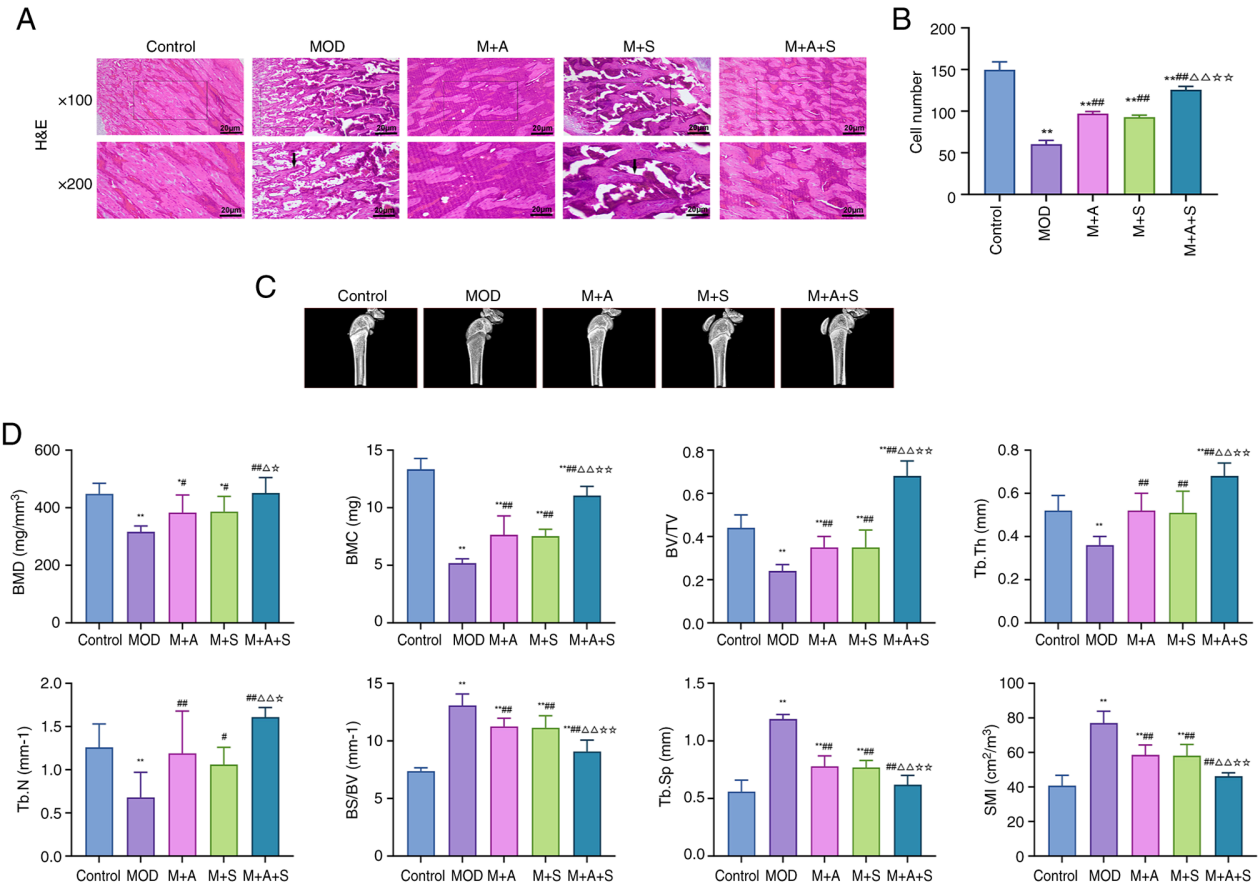

Figure 4. ASD and Semaglutide alleviate femoral damage in diabetic rats. (A and B) H&E staining was employed to examine femoral structure and count osteocytes and osteoblasts. (C and D) Micro-CT was adopted to assess trabecular microstructure of the femur and to perform quantitative analysis of related parameters. *P<0.05, **P<0.01 vs. Control; $^{\#}$P<0.05, $^{\#\#}$P<0.01 vs. MOD; $^{\Delta}$P<0.05, $^{\Delta\Delta}$P<0.01 vs. M + A; *P<0.05, **P<0.01 vs. M + S. ASD, akebia saponin D; H&E, hematoxylin and eosin; Micro-CT, micro-computed tomography.

were assessed. As shown in Fig. 5D-G, MOD rats displayed decreased levels of ALP and PINP and increased levels of CTX-I and TRAP. These changes indicate suppressed osteogenesis and enhanced bone resorption. Treatment with ASD or Semaglutide partially reversed these abnormalities, with M + A + S showing the most marked correction. At the

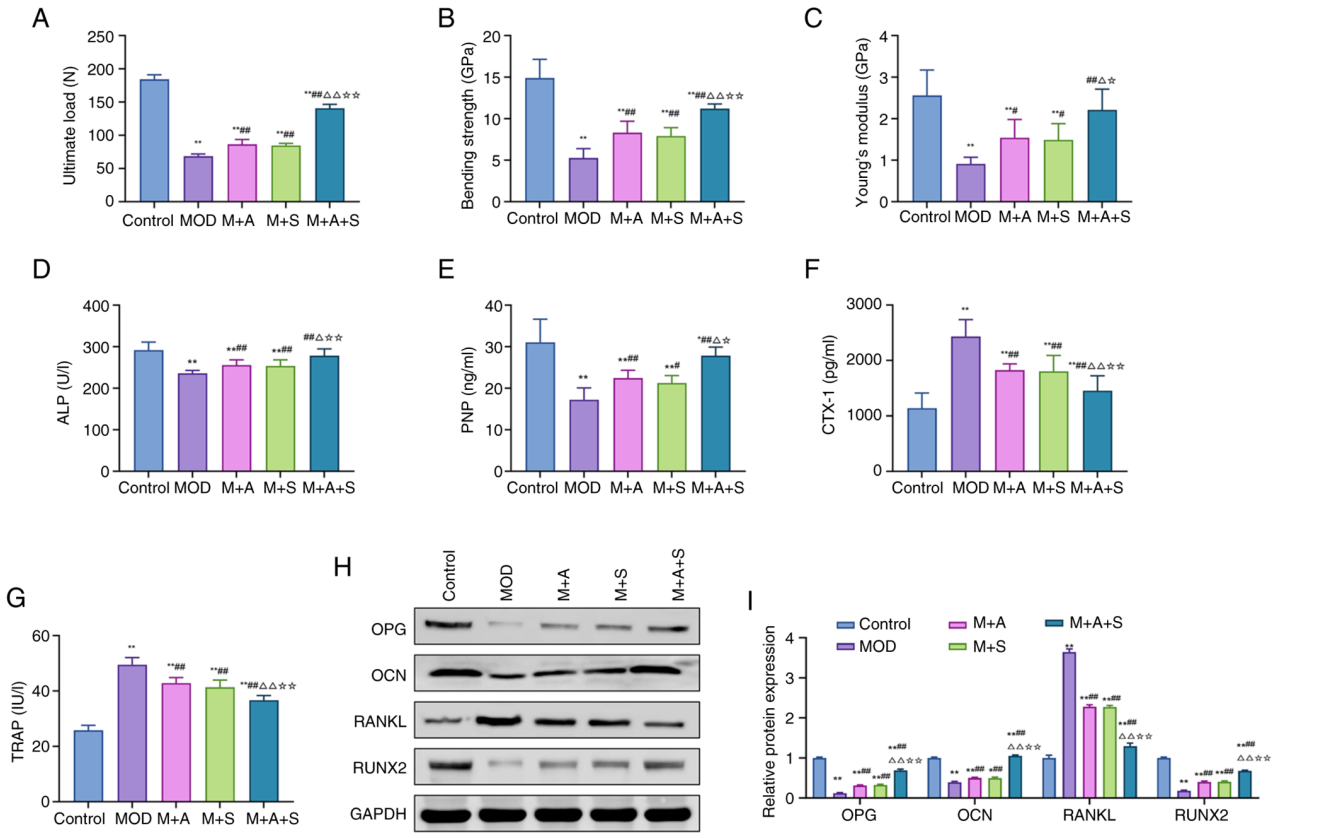

Figure 5. Effects of ASD and Semaglutide on bone metabolism and remodeling in diabetic rats. (A-C) Three-point bending tests measuring ultimate load, bending strength and Young's modulus of the femur. The serum levels of (D) ALP, (E) PINP, (F) CTX-1 and (G) TRAP were measured using ELISA. (H) Western blot and (I) quantification of femoral protein expression (OPG, OCN, RANKL and RUNX2). *P<0.05, **P<0.01 vs. Control; $^{\#}$P<0.05, $^{\#\#}$P<0.01 vs. MOD; $^{\triangle}$P<0.05, $^{\triangle\triangle}$P<0.01 vs. M + A; *P<0.05, **P<0.01 vs. M + S. ASD, akebia saponin D; ALP, alkaline phosphatase; PINP, procollagen type I N-terminal propeptide; CTX-1, C-terminal telopeptide of type I collagen; TRAP, tartrate-resistant acid phosphatase; OPG, osteoprotegerin; OCN, osteocalcin; RANKL, receptor activator of nuclear factor κ-b ligand; RUNX2, Runt-related transcription factor 2.

protein level (Fig. 5H and I), MOD rats exhibited reduced expression of OPG, OCN and RUNX2, along with upregulation of RANKL, a key stimulator of osteoclastogenesis. ASD and Semaglutide effectively normalized these markers, with combination therapy demonstrating the most pronounced modulation.

Together, these results indicated that the combined administration of ASD and Semaglutide enhances both bone mechanical integrity and metabolic homeostasis in DOP, probably by promoting osteogenesis and inhibiting bone resorption and achieves greater therapeutic efficacy than either agent alone.

Network pharmacology analysis of ASD and Semaglutide. After demonstrating the effectiveness of ASD and Semaglutide in treating DN and DOP, the present study used network pharmacology methods to further investigate their potential molecular targets and mechanisms. Through transcriptomic data analysis and KEGG enrichment analysis, the key molecules and signaling pathways were identified.

The transcriptomic datasets for DN (GSE30528) and OS (GSE35958) were both obtained from the GEO database. As shown in Fig. 6A and B, after differential expression analysis (adj. P<0.05; $|\log_2 FC| > 1$), 1,787 disease-related genes were identified. Drug-related targets of ASD and Semaglutide (n=252) were obtained from ChEMBL. Their intersection yielded 26 overlapping genes (Fig. 6C), which were used to construct a protein-protein interaction network (Fig. 6D), with TNF, PTEN and ESR1 emerging as central hub genes. GO enrichment analysis showed that these targets were involved in apoptotic signaling, oxidative stress response, MAPK cascade and calcium ion homeostasis (Fig. 6E-G). Cellular localization included neuronal compartments and membrane microdomains, while molecular functions encompassed chemokine binding, oxidoreductase and death domain activity. KEGG pathway analysis (Fig. 6H) revealed enrichment in p53 signaling, sphingolipid metabolism, T-cell receptor and apoptosis-related pathways, suggesting potential involvement of these signaling cascades in the pharmacological actions of ASD and Semaglutide.

These findings implied that ASD and Semaglutide may exert therapeutic effects via shared molecular targets involved in inflammation, apoptosis and cellular stress responses, with the p53 pathway emerging as a potential mechanistic link.

Molecular docking and expression analysis of Klotho in diabetic rats. Given the emerging role of Klotho in diabetic complications and its potential interaction with the p53 pathway (34), the present study explored whether ASD could directly bind to Klotho or p53 proteins using molecular docking. The binding energy of ASD with Klotho was-9.5 kcal/mol, while that with p53 was-7.6 kcal/mol, indicating a stronger affinity for Klotho (Fig. 7A and B).

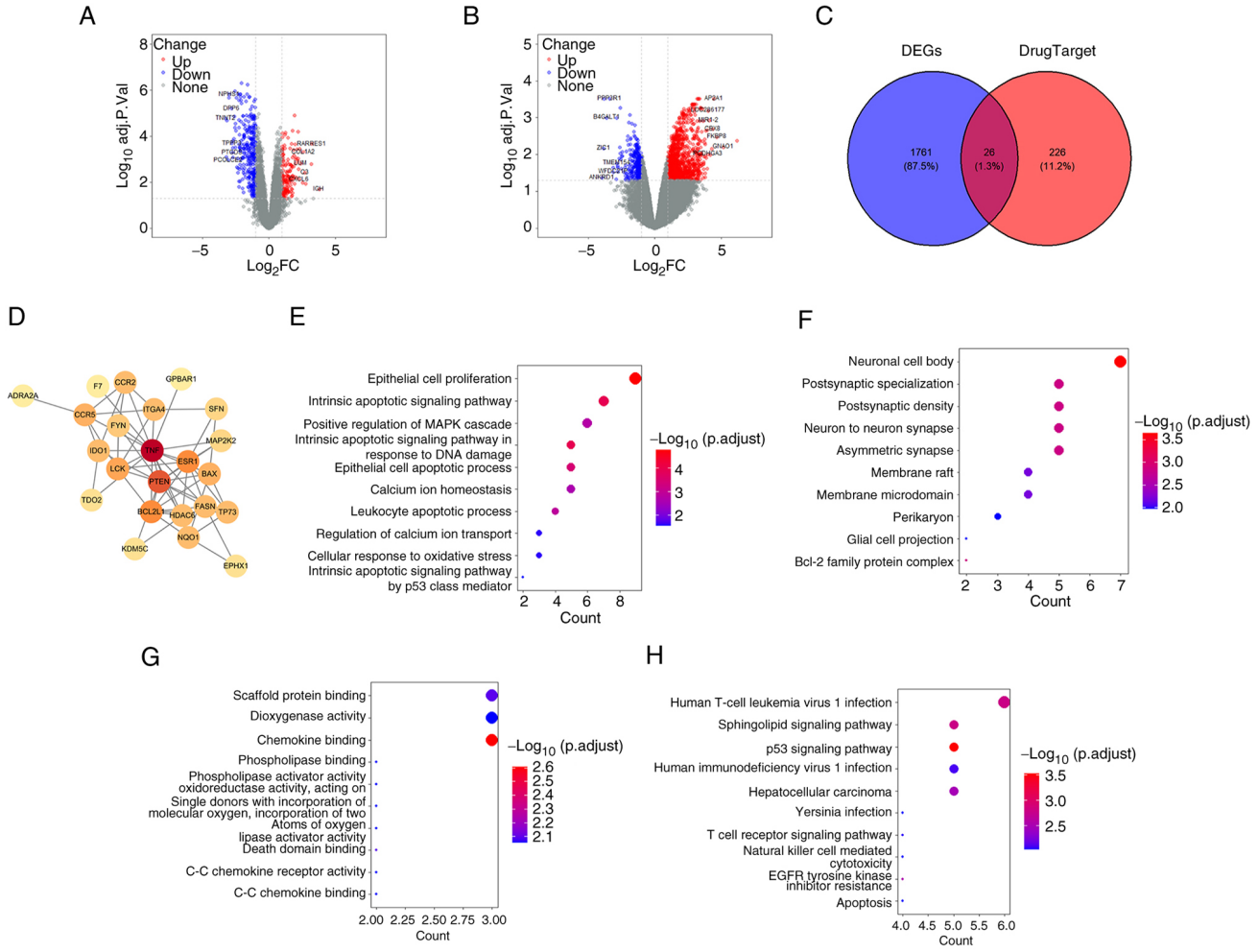

Figure 6. Network pharmacology analysis of ASD and Semaglutide. Identification of differentially expressed genes in the (A) GSE30528 and (B) GSE35958 datasets. (C) Venn diagram depicting the intersection of DEGs from both diseases and drug-related genes. (D) PPI network of 26 related genes. GO enrichment analysis for (E) biological process, (F) cellular component and (G) molecular function. (H) KEGG pathway enrichment analysis. ASD, akebia saponin D; DEGs, differentially expressed genes; PPI, protein-protein interaction; GO, Gene Ontology; KEGG, Kyoto Encyclopedia of Genes and Genomes.

Immunofluorescence and western blotting results showed that the Klotho protein level was markedly reduced in the kidney and femur tissues of rats in the MOD group, while treatment with ASD or Semaglutide markedly increased its expression, with the most pronounced effect observed in the M + A + S group (Fig. 7C-E).

These results implied that ASD may modulate the p53 pathway by targeting Klotho protein, thereby playing a role in the prevention of DN and DOP.

ASD and Semaglutide inhibit the p53 pathway and DNA damage in the kidney and femur tissues of diabetic rats. Abnormal activation of the p53 signaling pathway can lead to DNA damage, thereby exacerbating tissue injury (35). Therefore, the present study further investigated whether ASD and Semaglutide alleviated DN-related renal damage and DOP-related bone damage by inhibiting the p53 signaling pathway.

Immunofluorescence results (Fig. 8A and B) revealed markedly elevated levels of p53 and the DNA damage marker γ-H2AX in MOD rats. Treatment with ASD or Semaglutide reduced their expression, with the most pronounced suppression observed in the M + A + S group. Consistently, western blot analysis (Fig. 8C-F) showed upregulation of key proteins involved in DNA damage signaling, including ATM, p-ATM, p53, p21 and γ-H2AX, in MOD rats. All these markers were downregulated following ASD or Semaglutide treatment and combination therapy yielded the strongest inhibitory effect. These results suggested that combined treatment with ASD and Semaglutide could suppress the excessive activation of the p53 signaling pathway to reduce DNA damage, thereby exerting a protective effect in DN and DOP.

Knockdown of Klotho reverses the therapeutic effects of ASD and Semaglutide in diabetic nephropathy and diabetic osteoporosis. To further confirm whether Klotho served as a key target for the protective effects of ASD and Semaglutide, the present study applied AAV to knock down Klotho and observed its effect on the therapeutic outcomes.

Western blotting results confirmed successful Klotho knockdown in both kidney and femur tissues in M + A + S + sh-Klotho group (Figs. 9A and 10A). Functionally, renal injury indicators, including BUN, Cr, 24-up and renal index, were markedly elevated in the MOD group and attenuated by M + A + S treatment. However, these improvements were partially or fully reversed upon Klotho knockdown (Fig. 9B-E).

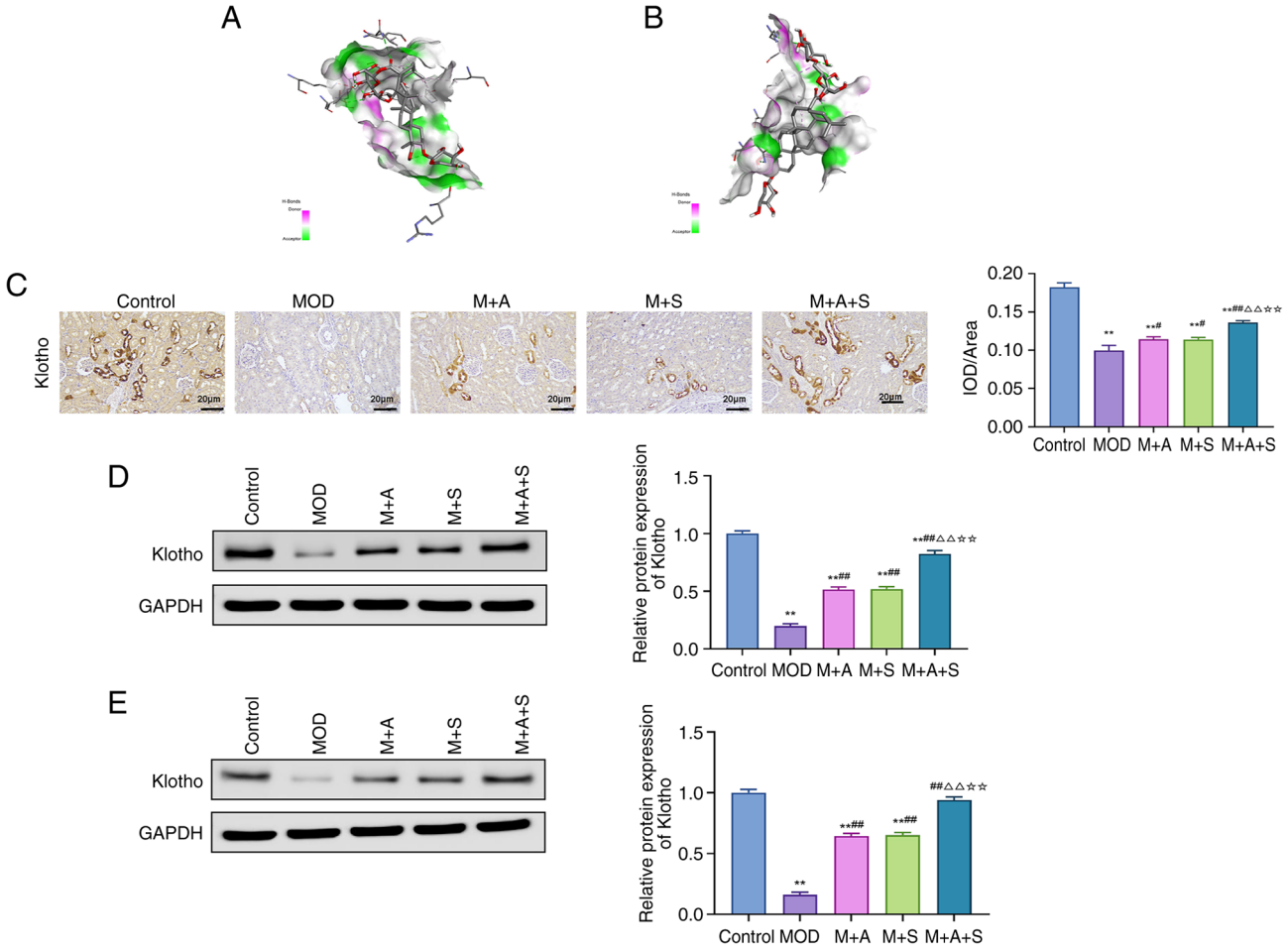

Figure 7. Molecular docking and expression analysis of Klotho in diabetic rats. Molecular docking models illustrating the interaction between ASD and (A) Klotho or (B) p53. (C) Immunohistochemical detection of Klotho levels in rat kidney tissues. Western blotting and quantitative analysis of Klotho protein levels in the (D) kidney and (E) femur. **P<0.01 vs. Control; $^{\#}$P<0.05, $^{\#\#}$P<0.01 vs. MOD; $^{\Delta\Delta}$P<0.01 vs. M + A; **P<0.01 vs. M + S. ASD, akebia saponin D.

Histopathological analysis (Fig. 9F-H) demonstrated that glomerular damage, basement membrane thickening and fibrosis, improved in the M + A + S group, were exacerbated again in the M + A + S + sh-Klotho group. Correspondingly, TGF-β1, α-SMA, Collagen I and IV expression levels were re-elevated (Fig. 9I and J), confirming that the anti-fibrotic effects of the therapy depended on Klotho expression.

In terms of the femur, trabecular structure improvements observed in the M + A + S group were abolished in sh-Klotho rats, with reduced osteoblast/osteocyte numbers and increased marrow cavity (Fig. 10B and C). Micro-CT analysis revealed that BMD improvements were also lost following Klotho knockdown (Fig. 10D). Moreover, the osteoanabolic proteins OPG, OCN and RUNX2 decreased again, while RANKL increased, indicating a shift back toward osteoclastic activation (Fig. 10 E and F).

Collectively, these results demonstrated that the therapeutic effects of ASD and Semaglutide on DN and DOP are Klotho-dependent, confirming Klotho as a critical mechanistic target.

Discussion

The present study indicated that co-administration of ASD and Semaglutide exerted significant therapeutic effects on both DN and DOP, potentially through modulation of the Klotho-p53 signaling axis. To the to the best of the authors' knowledge, the present study was the first to confirm the effect of ASD and Semaglutide combination therapy in DM complications and to elucidate the specific signaling pathways involved. Clinically, the present study provides a novel dual-target strategy for the comprehensive prevention and management of DM-associated complications. Since patients with DM often face both renal damage and osteoporosis, the combined therapy of ASD and Semaglutide may represent a highly valuable therapeutic strategy, potentially reducing damage to the kidney and skeletal systems while controlling blood glucose, which is of great importance for improving patient quality of life and prolonging lifespan.

The first challenge of the present study lies in how to establish an animal model that accurately reflects the characteristics of patients with T2DM with both DN and DOP in the real world. Although a high-fat, high-sugar diet combined with STZ injection is widely recognized as the primary method for constructing a DM animal model, the optimal STZ protocol remains a subject of debate (36). A single high-dose injection is generally regarded as mimicking T1DM, whereas multiple low-dose injections, when combined with dietary manipulation, are more often employed to simulate the progressive insulin resistance and partial β-cell dysfunction characteristic

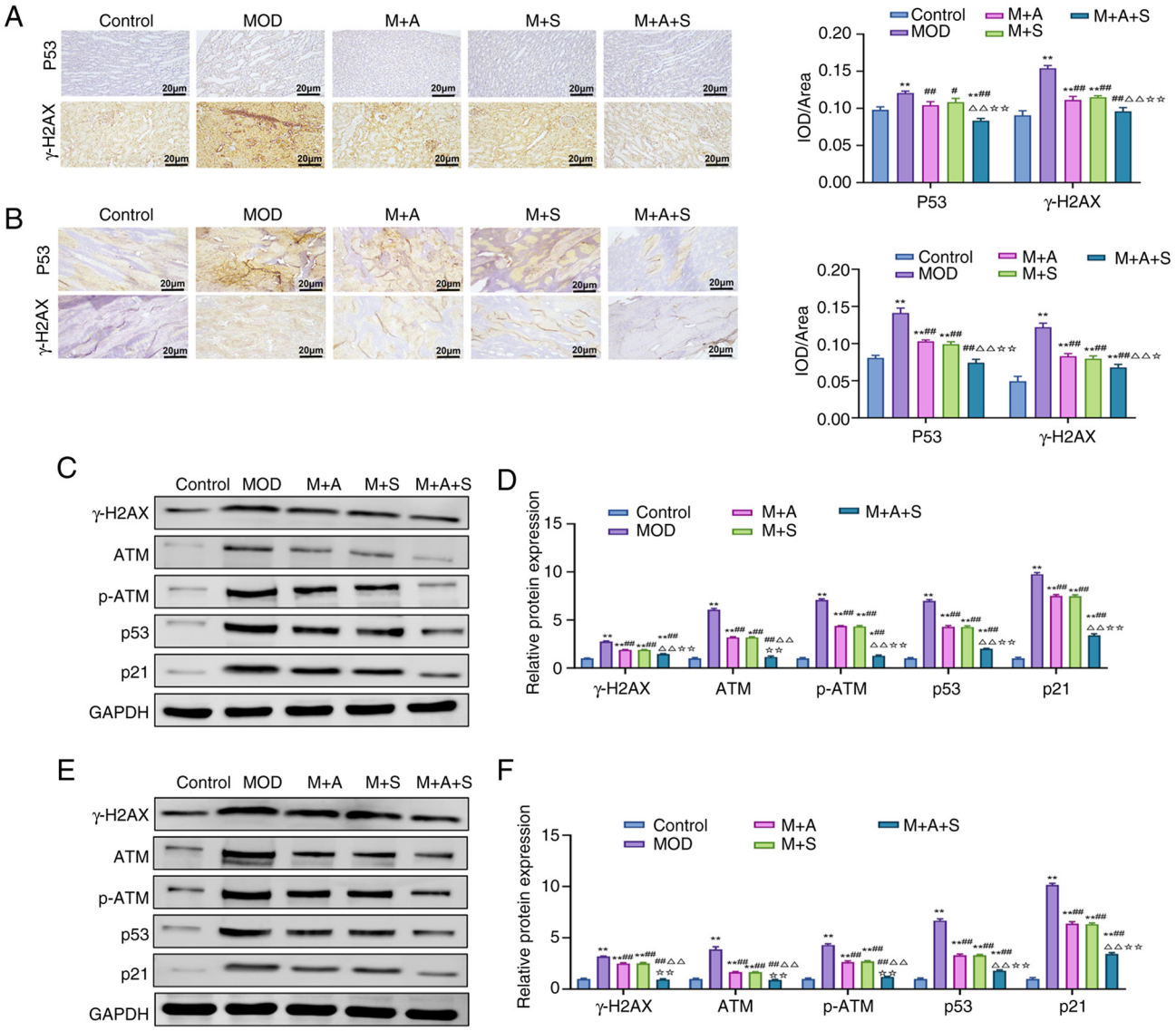

Figure 8. ASD and Semaglutide inhibit the p53 pathway and DNA damage in the kidney and femur tissues of diabetic rats. Immunohistochemical staining of p53 and γ-H2AX in (A) kidney and (B) femur tissues, respectively. (C-F) Western blotting and quantification analysis of DNA damage-related proteins, including γ-H2AX, ATM, p-ATM, p53 and p21, in (C and D) kidney and (E and F) femur tissues. *P<0.05, **P<0.01 vs. Control; $^{\#}$P<0.05, $^{\#\#}$P<0.01 vs. MOD; $^{\Delta\Delta}$P<0.01 vs. M + A; *P<0.05, **P<0.01 vs. M + S. ASD, akebia saponin D; p-, phosphorylated; ATM, ATM, ataxia-telangiectasia mutated protein.

of T2DM (33). The present study therefore adopted the latter approach, seeking to more closely approximate the clinical features of T2DM and its associated complications. Specifically, both single high-dose STZ injection and multiple low-dose STZ injections have been used in different studies. However, the mainstream view is that a single high-dose STZ injection (typically 50-75 mg/kg) directly destroys pancreatic β-cells, leading to absolute insulin deficiency and rapidly inducing hyperglycemia, simulating T1DM. By contrast, multiple low-dose STZ injections (typically 20-40 mg/kg per injection, sustained for more than 4 weeks) gradually destroy pancreatic β-cells and simulate the chronic process of insulin resistance and β-cell dysfunction, improved mimicking the pathological features of T2DM (37). Therefore, the present study adopted a high-fat, high-sugar diet combined with repeated low-dose STZ injections to attempt to establish a T2DM rat model. Comparing the MOD group rats with the Control group rats, it was found that the MOD group rats exhibited increased fasting blood glucose, elevated HOMA-IR, abnormal renal function indicators, destruction of kidney tissue structure, damage to femoral trabecular microstructure and reduced femoral biomechanical properties, thereby confirming that the MOD group rats exhibited both the kidney damage characteristics of DN and the bone damage characteristics of DOP. This provides a solid foundation for subsequent research.

The present study systematically evaluated the therapeutic synergy of ASD and Semaglutide from multiple perspectives. When examining the effects of the combined treatment of ASD and Semaglutide in alleviating DN kidney injury, the present study addressed three aspects: Serum and urine markers, kidney tissue structure and the degree of kidney fibrosis. First, it was found that after receiving ASD and Semaglutide combination therapy, the serum metabolic waste products BUN and Cr levels were markedly reduced in T2DM rats, indicating a recovery in kidney filtration function; 24-up levels decreased, suggesting an improvement in glomerular

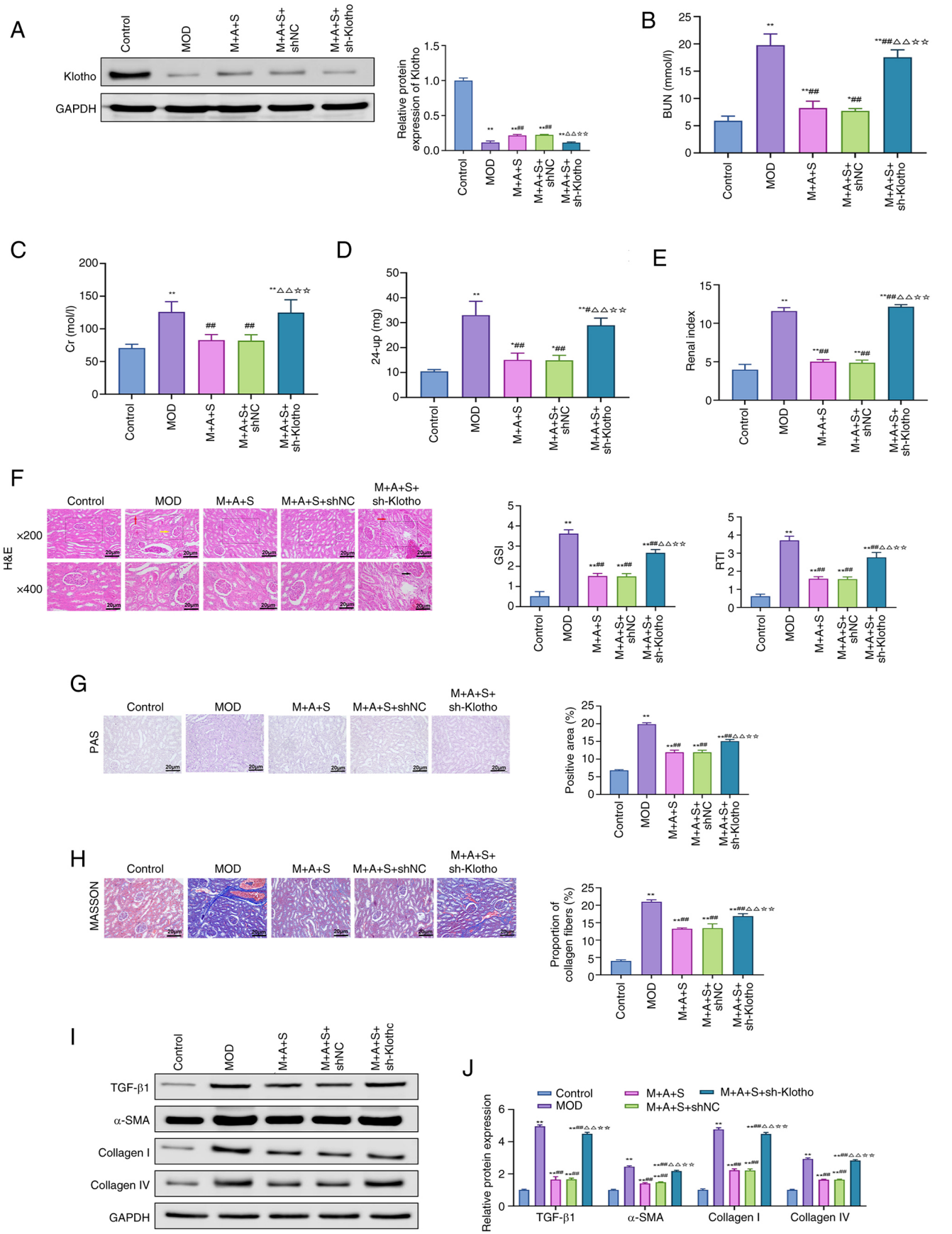

Figure 9. Klotho knockdown abrogates the renoprotective effects of ASD and Semaglutide. (A) Western blot analysis of Klotho protein levels in rat kidney tissues. (B-E) Serum levels of (B) BUN, (C) Cr, (D) 24-up and (E) kidney index. (F) H&E, (G) PAS and (H) Masson staining of renal tissue, with corresponding quantification of GSI, RTI, PAS-positive area and fibrosis index. (I) Western blotting and (J) quantification of renal TGF-β1, α-SMA, Collagen I and Collagen IV protein levels. *P<0.05, **P<0.01 vs. Control; $^{\#\#}$P<0.01 vs. MOD; $^{\triangle\triangle}$P<0.01 vs. M + A + S; **P<0.01 vs. M + A + S + shNC. ASD, akebia saponin D; BUN Cr, creatinine; 24-up, 24-h urinary protein; H&E, hematoxylin and eosin; PAS, periodic acid-Schiff; GSI, glomerulosclerosis index; RTI, renal tubular interstitial injury index; α-SMA, α-smooth muscle actin; sh, short hairpin.

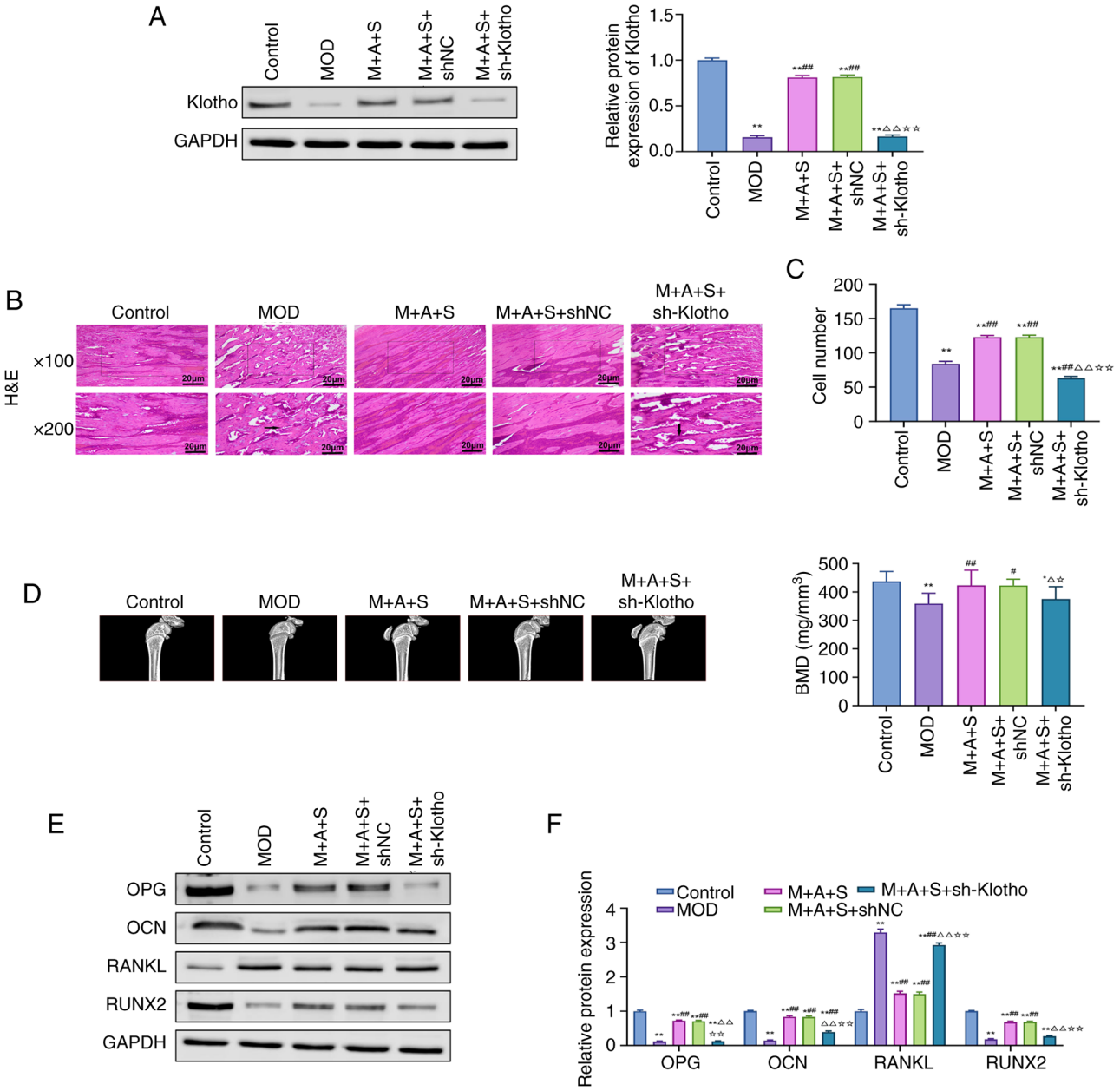

Figure 10. Knockdown of Klotho reverses the therapeutic effects of ASD and Semaglutide in the treatment of diabetic osteoporosis. (A) Western blot analysis of Klotho protein levels in rat femur tissue. (B and C) H&E staining to assess histological changes in rat femur tissues and cell counting of osteocytes and osteoblasts. (D) Micro-CT measurement of BMD in rat femur. (E and F) Western blot and quantification analysis of bone metabolic markers (OPG, OCN, RANKL and RUNX2). *P<0.05, **P<0.01 vs. Control; $^{\#}$P<0.05, $^{\#\#}$P<0.01 vs. MOD; $^{\Delta}$P<0.05, $^{\Delta\Delta}$P<0.01 vs. M + A + S; *P<0.05, **P<0.01 vs. M + A + S + shNC. ASD, akebia saponin D; H&E, hematoxylin and eosin; Micro-CT, micro-computed tomography; OPG, osteoprotegerin; OCN, osteocalcin; RANKL, receptor activator of nuclear factor κ-b ligand; RUNX2, Runt-related transcription factor 2.

barrier function; and the kidney index decreased, indicating alleviated kidney enlargement and congestion. Secondly, H&E staining visually showed reduced damage to the glomeruli and renal tubules; PAS staining showed decreased local deposition of glycation end products that directly damage the kidneys; and Masson staining reflected the inhibition of the kidney fibrosis process. Furthermore, combination therapy markedly downregulated TGF-β1, a key pro-fibrotic cytokine, as well as the major fibrotic matrix components α-SMA, Collagen I and Collagen IV (38), further confirming a significant improvement in kidney fibrosis. Lu *et al* (39) found that ASD slows DN progression by activating the NRF2/HO-1 pathway and inhibiting the NF-κB pathway and multiple studies have confirmed the anti-DN effects of Semaglutide (40,41), which are consistent with the findings of the present study.

When elucidating the effects of ASD combined with Semaglutide in alleviating DOP bone tissue damage, the present study also provided evidence from multiple perspectives. First, H&E staining clearly showed that the trabecular structure was markedly restored in T2DM rats following combined treatment. Second, micro-CT results indicated that the combined therapy markedly increased the trabecular health indicators BMD, BMC, BV/TV, Tb.Th and Tb.N, while markedly decreasing the trabecular rarity indicators BS/BV, Tb.Sp and SMI, suggesting an improvement in trabecular structure. Furthermore, three-point bending tests demonstrated that

the combined treatment markedly enhanced the mechanical strength and stability of T2DM rat bones. Last, following combined treatment, osteogenesis-related biomarkers such as ALP, PINP, OPG, OCN and RUNX2 were markedly elevated, while bone resorption-related markers, including CTX-1, TRAP and RANKL, were markedly decreased (42), further confirming the osteogenic and anti-osteoporotic effects of ASD and Semaglutide. Previous studies have shown that Semaglutide improves bone metabolism in patients with DM (43,44), which is consistent with our findings. However, limited research has explored whether ASD can improve bone quality, making this one of the significant innovations of our study.

Importantly, to clarify the interdependency of renal and skeletal protection, the present study investigated whether ASD and Semaglutide synergistically attenuated the progression of both DM-related complications and further examined calcium and phosphorus metabolism in T2DM rats. Previous studies have shown that dysregulation of calcium-phosphorus metabolism is a key factor in the mutual aggravation of DN and DOP. Specifically, during DN progression, tubular damage often leads to phosphate retention and hyperphosphatemia, which suppresses osteoblast activity and calcium absorption, ultimately exacerbating osteoporosis. Conversely, as bone tissue serves as a reservoir for calcium and phosphate, disturbances in bone metabolism can result in excessive phosphate release, increasing the burden on renal excretion and accelerating renal dysfunction and DN progression (45,46). The present study showed that combined ASD and Semaglutide treatment markedly reduced serum phosphate levels, decreased urinary calcium and phosphate excretion and enhanced bone mineralization, thereby alleviating calcium-phosphorus metabolic disorders and playing a critical role in the simultaneous protection of kidney and bone health.

Upon confirming the dual efficacy of ASD and Semaglutide in ameliorating DN and DOP, the present study further investigated the potential molecular mechanisms, with a focus on the Klotho-p53 signaling axis. Klotho was initially identified as an anti-aging protein highly expressed in renal distal tubules and the choroid plexus of the brain (47). Subsequent studies revealed that soluble Klotho is widely present in urine, blood and cerebrospinal fluid and participates in multiple physiological processes by regulating various intracellular signaling pathways, including insulin/IGF-1, p53 and Wnt (48,49). Aberrant Klotho expression is now recognized as a hallmark of DM (50,51). Nie *et al* (52) reported markedly lower serum Klotho levels in patients with DM compared with healthy controls, with levels declining further as disease duration increased. Similarly, Kim *et al* (53) found that serum Klotho may serve as an early predictor of DN risk. Among the proteins regulated by Klotho, p53 is particularly relevant to DM. While p53 normally maintains oxidative balance by upregulating antioxidant genes, its role in DM is largely deleterious, contributing to disease progression (54). p53 can induce β-cell DNA damage, promote β-cell apoptosis, inhibit glucose transport and glycolysis, promote gluconeogenesis and downregulate insulin receptor expression, all contributing to insulin resistance and DM progression (55). Based on this, it was hypothesized that upregulation of Klotho to suppress p53 signaling may represent a key mechanism underlying the therapeutic effects of ASD and Semaglutide. To test this, the present study first conducted a bioinformatics analysis. Among 1,787 DN/DOP-related targets and 246 ASD/Semaglutide-related targets, multiple Klotho-p53 axis-associated molecules were enriched, with KEGG pathway analysis highlighting the p53 pathway. Furthermore, molecular docking showed strong interactions between ASD and both Klotho and p53, with low binding energies. *In vivo*, combined ASD and Semaglutide therapy markedly increased Klotho protein levels and reduced p53 expression in renal and femoral tissues, while Klotho knockdown attenuated their protective effects, supporting the hypothesis that the Klotho-p53 axis mediates their therapeutic action.

Nevertheless, the optimal dosing strategy and long-term safety of this combination therapy require further evaluation. Specifically, the present study did not investigate dose-response relationships or potential adverse effects associated with prolonged administration of ASD and Semaglutide. This limitation restricts the immediate clinical application of the therapy and future studies should therefore focus on optimizing dosing regimens, monitoring toxicity profiles and conducting long-term safety assessments in both preclinical and clinical settings. In addition, several limitations of the present study should be acknowledged. First, the research was conducted in a rat model of T2DM, which may not fully replicate the complexity of human diabetic nephropathy and osteoporosis and therefore the translational relevance should be interpreted with caution. Second, the sample size was relatively modest, which may limit the statistical power to detect subtle effects. Third, although the present study focused on the Klotho-p53 signaling axis, other molecular pathways could also contribute to the observed therapeutic benefits and further mechanistic exploration is warranted. Finally, the present study did not include long-term follow-up or clinical validation and thus the efficacy and safety of ASD combined with Semaglutide need to be confirmed in larger preclinical studies and clinical trials.

In summary, the present study demonstrates that the natural small-molecule compound ASD and the long-acting GLP-1 receptor agonist Semaglutide exert a significant synergistic effect in the treatment of DN and DOP, with superior efficacy compared with either agent alone. Mechanistically, their combined action in mitigating DM-related complications is likely mediated through modulation of the Klotho-p53 signaling axis. These findings offer new insights into the prevention and treatment of DM-associated complications.

Acknowledgements

Not applicable.

Funding

The present study was supported by the National Natural Science Foundation of China (grant no. 82270862) and the Guangdong Basic and Applied Basic Research Foundation (grant no. 2024A1515220024).

Availability of data and materials

The data generated in the present study may be requested from the corresponding author.

Authors' contributions

QZ was responsible for conceptualization, investigation, formal analysis and writing the original draft. DW was responsible for methodology, data curation, validation and visualization. HXJ was responsible for investigation, resources and data curation. DW and HXJ confirm the authenticity of all the raw data. ZJZ was responsible for investigation, software and formal analysis. LYL was responsible for methodology, histological analysis and western blotting. LNL was responsible for investigation, immunofluorescence and micro-CT analysis. LW was responsible for software, bioinformatics analysis, molecular docking, writing, reviewing and editing. YMX was responsible for conceptualization, supervision, project administration, writing the original draft, writing, reviewing and editing. All authors read and approved the final manuscript.

Ethics approval and consent to participate

Ethical approval for the present study was obtained from the Animal Welfare and Ethics Committee of Guangdong Medical Laboratory Animal Center (approval no. D202505-13).

Patient consent for publication

Not applicable.

Competing interests

The authors declare that they have no competing interests.

Authors' information

Dr Yaoming Xue
ORCID: 0000-0003-1356-4780

References

1. Yang T, Qi F, Guo F, Shao M, Song Y, Ren G, Linlin Z, Qin G and Zhao Y: An update on chronic complications of diabetes mellitus: From molecular mechanisms to therapeutic strategies with a focus on metabolic memory. Mol Med 30: 71, 2024.
2. Lovic D, Piperidou A, Zografou I, Grassos H, Pittaras A and Manolis A: The growing epidemic of diabetes mellitus. Curr Vasc Pharmacol 18: 104-109, 2020.
3. Saeedi P, Petersohn I, Salpea P, Malanda B, Karuranga S, Unwin N, Colagiuri S, Guariguata L, Motala AA, Ogurtsova K, *et al*: Global and regional diabetes prevalence estimates for 2019 and projections for 2030 and 2045: Results from the International Diabetes Federation Diabetes Atlas, 9th edition. Diabetes Res Clin Pract 157: 107843, 2019.
4. Magee C, Grieve DJ, Watson CJ and Brazil DP: Diabetic nephropathy: A tangled web to unweave. Cardiovasc Drugs Ther 31: 579-592, 2017.
5. Thipsawat S: Early detection of diabetic nephropathy in patient with type 2 diabetes mellitus: A review of the literature. Diab Vasc Dis Res 18: 14791641211058856, 2021.
6. Bao K, Jiao Y, Xing L, Zhang F and Tian F: The role of wnt signaling in diabetes-induced osteoporosis. Diabetol Metab Syndr 15: 84, 2023.
7. Vestergaard P: Discrepancies in bone mineral density and fracture risk in patients with type 1 and type 2 diabetes-a meta-analysis. Osteoporos Int 18: 427-444, 2007.
8. Janghorbani M, Van Dam RM, Willett WC and Hu FB: Systematic review of type 1 and type 2 diabetes mellitus and risk of fracture. Am J Epidemiol 166: 495-505, 2007.
9. Wang J, You W, Jing Z, Wang R, Fu Z and Wang Y: Increased risk of vertebral fracture in patients with diabetes: A meta-analysis of cohort studies. Int Orthop 40: 1299-1307, 2016.
10. Xia J, Zhong Y, Huang G, Chen Y, Shi H and Zhang Z: The relationship between insulin resistance and osteoporosis in elderly male type 2 diabetes mellitus and diabetic nephropathy. Ann Endocrinol (Paris) 73: 546-551, 2012.
11. Yan P, Xu Y, Zhang Z, Zhu J, Miao Y, Gao C and Wan Q: Association of circulating Omentin-1 with Osteoporosis in a Chinese Type 2 diabetic population. Mediators Inflamm 2020: 9389720, 2020.
12. Yang S, Hu T, Liu H, Lv YL, Zhang W, Li H, Xuan L, Gong LL and Liu LH: Akebia saponin D ameliorates metabolic syndrome (MetS) via remodeling gut microbiota and attenuating intestinal barrier injury. Biomed Pharmacother 138: 111441, 2021.
13. Xuan L, Yang S, Ren L, Liu H, Zhang W, Sun Y, Xu B, Gong L and Liu L: Akebia saponin D attenuates allergic airway inflammation through AMPK activation. J Nat Med 78: 393-402, 2024.
14. Gu L, Ye L, Chen Y, Deng C, Zhang X, Chang J, Feng M, Wei J, Bao X and Wang R: Integrating network pharmacology and transcriptomic omics reveals that akebia saponin D attenuates neutrophil extracellular Traps-induced neuroinflammation via NTSR1/PKAc/PAD4 pathway after intracerebral hemorrhage. FASEB J 38: e23394, 2024.
15. Gong LL, Yang S, Zhang W, Han FF, Lv YL, Wan ZR, Liu H, Jia YJ, Xuan LL and Liu LH: Akebia saponin D alleviates hepatic steatosis through BNip3 induced mitophagy. J Pharmacol Sci 136: 189-195, 2018.
16. Kristensen SL, Rorth R, Jhund PS, Docherty KF, Sattar N, Preiss D, Køber L, Petrie MC and McMurray JJV: Cardiovascular, mortality, and kidney outcomes with GLP-1 receptor agonists in patients with type 2 diabetes: A systematic review and meta-analysis of cardiovascular outcome trials. Lancet Diabetes Endocrinol 7: 776-785, 2019.
17. Yao H, Zhang A, Li D, Wu Y, Wang CZ, Wan JY and Yuan CS: Comparative effectiveness of GLP-1 receptor agonists on glycaemic control, body weight, and lipid profile for type 2 diabetes: Systematic review and network meta-analysis. BMJ 384: e076410, 2024.
18. Beery AK and Zucker I: Sex bias in neuroscience and biomedical research. Neurosci Biobehav Rev 35: 565-572, 2011.
19. Mauvais-Jarvis F: Sex differences in metabolic homeostasis, diabetes, and obesity. Biol Sex Differ 6: 14, 2015.
20. Du J, Zhu M, Li H, Liang G, Li Y and Feng S: Metformin attenuates cardiac remodeling in mice through the Nrf2/Keap1 signaling pathway. Exp Ther Med 20: 838-845, 2020.
21. O'Neil PM, Birkenfeld AL, McGowan B, Mosenzon O, Pedersen SD, Wharton S, Carson CG, Jepsen CH, Kabisch M and Wilding JPH: Efficacy and safety of semaglutide compared with liraglutide and placebo for weight loss in patients with obesity: A randomised, Double-blind, placebo and active controlled, dose-ranging, phase 2 trial. Lancet 392: 637-649, 2018.
22. Davies M, Faerch L, Jeppesen OK, Pakseresht A, Pedersen SD, Perreault L, Rosenstock J, Shimomura I, Viljoen A, Wadden TA, *et al*: Semaglutide 2.4 mg once a week in adults with overweight or obesity, and type 2 diabetes (STEP 2): A randomised, double-blind, double-dummy, placebo-controlled, phase 3 trial. Lancet 397: 971-984, 2021.
23. Nair AB and Jacob S: A simple practice guide for dose conversion between animals and human. J Basic Clin Pharm 7: 27-31, 2016.
24. Huang KC, Chuang PY, Yang TY, Tsai YH, Li YY and Chang SF: Diabetic rats induced using a High-fat diet and Low-dose streptozotocin treatment exhibit gut microbiota dysbiosis and osteoporotic bone pathologies. Nutrients 16: 1220, 2024.
25. Srinivasan K, Viswanad B, Asrat L, Kaul CL and Ramarao P: Combination of high-fat diet-fed and low-dose streptozotocin-treated rat: A model for type 2 diabetes and pharmacological screening. Pharmacol Res 52: 313-320, 2005.
26. Liu MM, Dong R, Hua Z, Lv NN, Ma Y, Huang GC, Cheng J and Xu HY: Therapeutic potential of liuwei dihuang pill against KDM7A and Wnt/β-catenin signaling pathway in diabetic nephropathy-related osteoporosis. Biosci Rep 40: BSR20201778, 2020.
27. Yu X, Wang LN, Du QM, Ma L, Chen L, You R, Liu L, Ling JJ, Yang ZL and Ji H: Akebia Saponin D attenuates amyloid β-induced cognitive deficits and inflammatory response in rats: Involvement of Akt/NF-κB pathway. Behav Brain Res 235: 200-209, 2012.

28. Cardiff RD, Miller CH and Munn RJ: Manual hematoxylin and eosin staining of mouse tissue sections. Cold Spring Harb Protoc 2014: 655-658, 2014.
29. Gu LY, Yun S, Tang HT and Xu ZX: Huangkui capsule in combination with metformin ameliorates diabetic nephropathy via the Klotho/TGF-beta1/p38MAPK signaling pathway. J Ethnopharmacol 281: 113548, 2021.
30. Yaroslavceva MV, Bondarenko ON, El-Taravi YA, Magerramova ST, Pigarova EA, Ulyanova IN and Galstyan GR: (Etiopathogenetic features of bone metabolism in patients with diabetes mellitus and Charcot foot). Probl Endokrinol (Mosk) 70: 57-64, 2024 (In Russian).
31. Ma R, Zhu R, Wang L, Guo Y, Liu C, Liu H, Liu F, Li H, Li Y, Fu M and Zhang D: Diabetic osteoporosis: A review of its traditional Chinese medicinal use and clinical and preclinical research. Evid Based Complement Alternat Med 2016: 3218313, 2016.
32. Chen F, Wang P, Dai F, Zhang Q, Ying R, Ai L and Chen Y: Correlation between blood glucose fluctuations and osteoporosis in type 2 diabetes mellitus. Int J Endocrinol 2025: 8889420, 2025.
33. Ishtaya GA, Anabtawi YM, Zyoud SH and Sweileh WM: Osteoporosis knowledge and beliefs in diabetic patients: A cross sectional study from Palestine. BMC Musculoskelet Disord 19: 43, 2018.
34. Prud'homme GJ and Wang Q: Anti-Inflammatory role of the klotho protein and relevance to aging. Cells 13, 1413, 2024.
35. Marei HE, Althani A, Afifi N, Hasan A, Caceci T, Pozzoli G, Morrione A, Giordano A and Cenciarelli C: p53 signaling in cancer progression and therapy. Cancer Cell Int 21: 703, 2021.
36. Goyal SN, Reddy NM, Patil KR, Nakhate KT, Ojha S, Patil CR and Agrawal YO: Challenges and issues with streptozotocin-induced diabetes-A clinically relevant animal model to understand the diabetes pathogenesis and evaluate therapeutics. Chem Biol Interact 244: 49-63, 2016.
37. Rais N, Ved A, Ahmad R, Parveen K, Gautam GK, Bari DG, Shukla KS, Gaur R and Singh AP: Model of Streptozotocin-nicotinamide induced type 2 diabetes: A comparative review. Curr Diabetes Rev 18: e171121198001, 2022.
38. Klinkhammer BM and Boor P: Kidney fibrosis: Emerging diagnostic and therapeutic strategies. Mol Aspects Med 93: 101206, 2023.
39. Lu C, Fan G and Wang D: Akebia Saponin D ameliorated kidney injury and exerted anti-inflammatory and anti-apoptotic effects in diabetic nephropathy by activation of NRF2/HO-1 and inhibition of NF-KB pathway. Int Immunopharmacol 84: 106467, 2020.
40. Moellmann J, Klinkhammer BM, Onstein J, Stöhr R, Jankowski V, Jankowski J, Lebherz C, Tacke F, Marx N, Boor P and Lehrke M: Glucagon-Like peptide 1 and its cleavage products are renoprotective in murine diabetic nephropathy. Diabetes 67: 2410-2419, 2018.
41. Veneti S and Tziomalos K: Is there a role for glucagon-like peptide-1 receptor agonists in the management of diabetic nephropathy? World J Diabetes 11: 370-373, 2020.
42. Fernandez-Villabrille S, Martin-Carro B, Martin-Virgala J, Rodríguez-Santamaria MDM, Baena-Huerta F, Muñoz-Castañeda JR, Fernández-Martín JL, Alonso-Montes C, Naves-Díaz M, Carrillo-López N and Panizo S: Novel biomarkers of bone metabolism. Nutrients 16: 605, 2024.
43. Onoviran OF, Li D, Toombs Smith S and Raji MA: Effects of glucagon-like peptide 1 receptor agonists on comorbidities in older patients with diabetes mellitus. Ther Adv Chronic Dis 10: 2040622319862691, 2019.
44. Herrou J, Mabilleau G, Lecerf JM, Thomas T, Biver E and Paccou J: Narrative review of effects of Glucagon-like Peptide-1 receptor agonists on bone health in people living with obesity. Calcif Tissue Int 114: 86-97, 2024.
45. Sun M, Wu X, Yu Y, Wang L, Xie D, Zhang Z, Chen L, Lu A, Zhang G and Li F: Disorders of calcium and phosphorus metabolism and the Proteomics/Metabolomics-Based research. Front Cell Dev Biol 8: 576110, 2020.
46. Winiarska A, Filipska I, Knysak M and Stompor T: Dietary phosphorus as a marker of mineral metabolism and progression of diabetic kidney disease. Nutrients 13: 789, 2021.
47. Buchanan S, Combet E, Stenvinkel P and Shiels PG: Klotho, Aging, and the failing kidney. Front Endocrinol (Lausanne) 11: 560, 2020.
48. Hosseini L, Babaie S, Shahabi P, Fekri K, Shafiee-Kandjani AR, Mafikandi V, Maghsoumi-Norouzabad L and Abolhasanpour N: Klotho: Molecular mechanisms and emerging therapeutics in central nervous system diseases. Mol Biol Rep 51: 913, 2024.
49. Kanbay M, Copur S, Ozbek L, Mutlu A, Cejka D, Ciceri P, Cozzolino M and Haarhaus ML: Klotho: A potential therapeutic target in aging and neurodegeneration beyond chronic kidney disease-a comprehensive review from the ERA CKD-MBD working group. Clin Kidney J 17: sfad276, 2024.
50. Tang A, Zhang Y, Wu L, Lin Y, Lv L, Zhao L, Xu B, Huang Y and Li M: Klotho's impact on diabetic nephropathy and its emerging connection to diabetic retinopathy. Front Endocrinol (Lausanne) 14: 1180169, 2023.
51. Hejrati A, Zabihi T, Riazi S and Sarv F: Klotho: A possible diagnostic biomarker and therapeutic target in diabetes complications. Int J Diabetes Developing Countries: 1-16, 2025.
52. Nie F, Wu D, Du H, Yang X, Yang M, Pang X and Xu Y: Serum klotho protein levels and their correlations with the progression of type 2 diabetes mellitus. J Diabetes Complications 31: 94-98, 2017.
53. Kim SS, Song SH, Kim IJ, Lee EY, Lee SM, Chung CH, Kwak IS, Lee EK and Kim YK: Decreased plasma alpha-Klotho predict progression of nephropathy with type 2 diabetic patients. J Diabetes Complications 30: 887-892, 2016.
54. Lahalle A, Lacroix M, De Blasio C, Cisse MY, Linares LK and Le Cam L: The p53 Pathway and Metabolism: The tree that hides the forest. Cancers (Basel) 13: 133, 2021.
55. Kung CP and Murphy ME: The role of the p53 tumor suppressor in metabolism and diabetes. J Endocrinol 231: R61-R75, 2016.